Pion Production by 185-MeV Protons*

Michael P. Keating† and John G. Wills

Indiana University, Bloomington, Indiana 47401

(Received 2 October 1972)

We present distorted-wave Born-approximation calculations of the reaction $^{12}C(p, \pi^+)^{13}C$ at $T_p = 185$ MeV. It is found that the production cross section to specific states in ^{13}C depends very sensitively on the pion-nucleus distorted-wave function.

We consider a distorted-wave Born-approximation (DWBA) calculation of the differential cross sections for $^{12}C(p, \pi^+)^{13}C$ at $T_p = 185$ MeV and ^{13}C being left in either the ground state or in one of the excited states between 3- and 4-MeV excitation energy.

The differential cross section for this reaction is given by first-order time-dependent perturbation theory as

$$\sigma(\vec{K}_\pi, \vec{K}_p) = \frac{1}{(2\pi)^2} \frac{K_\pi}{K_p} \frac{E_\pi E_p}{2} \sum_{i,f} |\langle f|H'|i\rangle|^2 ,$$

where $K_\pi(E_\pi)$ and $K_p(E_p)$ are the pion and proton momenta (relativistic energies). The sum is over the spin projection of the incident nucleon, and the total angular momentum projection of the residual nucleus. (The units are such that $\hbar = c = 1$.) The transition operator employed here is the usual Galilean invariant form of the pion-nucleon interaction

$$H' = \sqrt{4\pi}\, \frac{f}{\mu}\, i[\vec{\sigma} \cdot \vec{\nabla}_\pi(\vec{\tau} \cdot \vec{\Phi}) - \frac{\mu}{m}(\vec{\tau} \cdot \vec{\Phi})\vec{\sigma} \cdot \vec{\nabla}_p] ,$$

where f is the pion-nucleon coupling constant ($f^2 = 0.088$), $\vec{\sigma}$ and $\vec{\tau}$ are the nucleon spin and isospin Pauli matrices, μ and m are the pion and proton mass, respectively, and $\vec{\Phi}$ is the pion field (which is treated as a vector in isospin space). $\vec{\nabla}_\pi$ acts only on the pion field directly to its right, and $\vec{\nabla}_p$ acts only on the incident proton's coordinates. The matrix element of $\vec{\tau} \cdot \vec{\Phi}$ between a final state consisting of one positive pion of momentum K_π, and an initial state consisting of the vacuum is

$$\langle K_\pi + |\vec{\tau} \cdot \vec{\Phi}|0\rangle = \left(\frac{1}{2E_\pi}\right)^{1/2} \chi^{(-)*}(\vec{K}_\pi, \vec{r}_\pi)\tau_- ,$$

where τ_- is the nucleon-isospin-lowering operator, and $\chi^{(-)*}(\vec{K}_\pi, \vec{r}_\pi)$ is the pion wave function. After summing over the nucleon-isospin coordinates,

we obtain the matrix element $\langle f|H'|i\rangle$ as

$$\langle f|H'|i\rangle = \sqrt{4\pi}\, \frac{f}{\mu}\, \frac{1}{\sqrt{2E_\pi}}\, \langle \Psi_{JM}|\vec{\sigma} \cdot \vec{\nabla}_\pi \chi^{(-)*}(\vec{K}_\pi, \vec{r}_\pi) - \frac{\mu}{m}\chi^{(-)*}(\vec{K}_\pi, \vec{r}_\pi)\vec{\sigma} \cdot \vec{\nabla}_p | \Psi_0, \, \psi_m(\vec{K}_p, \vec{r}_p, \vec{\sigma}_p)\rangle ,$$

where Ψ_{JM} and Ψ_0 are the wave functions for the residual and target nuclei. $\psi_m(K_p, r_p, \sigma_p)$ represents the incident proton. σ_p is the spin variable, and m is the initial spin projection. The radial dependence of the nuclear matrix element is taken to be the radial bound-state wave function of the (transferred) neutron.

We used standard, local optical-model wave functions for the proton distorted wave. Spin-orbit coupling was included. The Coulomb interaction was described by a potential representing a uniform charge distribution of radius r_c. The real part of the central potential was $V_{cR} = V_u f(r, R_u, a_u)$, where the function $f(r, R, a) = (1 + e^{(r-R)/a})^{-1}$. The imaginary part of the central potential was $V_{cI} = V_I f(r, R_I, a_I)$, and the spin-orbit potential was $V_{1j} = (V_s + i\, W_s)2/r[-(d/dr)f(r, R_s, a_s)]\vec{l} \cdot \vec{\sigma}$. We used potential parameters which give best fits to

185-MeV elastic scattering data. They were[1] $V_u = -16$ MeV, $R_u = 1.0A^{1/3}$ fm, $a_u = 0.5$, $V_I = -10$ MeV, $R_I = 1.34A^{1/3}$ fm, $a_I = 0.5$, $V_s = -2.5$ MeV, $W_s = 1.0$ MeV, $R_s = 1.0A^{1/3}$ fm, $a_s = 0.5$, and $r_c = 1.26A^{1/3}$ fm.

For the pion distorted waves, we originally used the Kroll-Kisslinger pion optical model.[2,3] The equation is

$$\{\nabla^2 + [(E_\pi - V_{Cou})^2 - \mu^2]\} \chi(\vec{K}_\pi, \vec{r}_\pi)$$

$$= \{-b_0 K_\pi^2 \rho(r) + \vec{\nabla} \cdot b_1 \rho(r)$$

$$\times [1 + \tfrac{1}{3}\xi b_1 \rho(r)]^{-1}\vec{\nabla}\} \chi(\vec{K}_\pi, \vec{r}_\pi),$$

where V_{Cou} is the Coulomb potential, and $\rho(r)$ is the nucleon density normalized to the number of nucleons. Since no π^+-^{13}C elastic scattering data exists, we used π^+-^{12}C potential parameters, and

assumed the A dependence is mostly contained in the normalization to the number of nucleons. The density used was $\rho(r) = N(1 + Wr^2/a^2)\,e^{-r^2/a^2}$, where N is the normalization constant, $W = \frac{4}{3}$, and $a = 1.6$ fm. The Coulomb potential was calculated from a modified Gaussian charge density normalized to the nuclear charge. The parameters were $W = \frac{4}{3}$, and $a = 1.55$ fm. For 185-MeV protons incident on ^{12}C, the resulting pion has a center-of-mass kinetic energy of 33.1 MeV when ^{13}C is left in the ground state. We used best-fit parameters to 30.2-MeV π^+-^{12}C elastic scattering. They are $b_0 = -4.45 + i\,0.669$ and $b_1 = 7.20 + i\,0.465$ for $\xi = 1$[6]; and $b_0 = -4.41 + i\,0.140$ and $b_1 = 5.26 + i\,0.180$ for $\xi = 0$.[4]

The neutron's bound-state wave function was calculated with the usual Schrödinger equation. A Woods-Saxon potential was used, and the radius parameter was varied to test the sensitivity of the pion-production results. The depth was adjusted to give the correct neutron-separation energy. The diffuseness parameter used was 0.5, and the radius parameter was varied from $R_n = 1.22A^{1/3}$ fm to $R_n = 1.31A^{1/3}$ fm. (We used $A = 12$ here.)

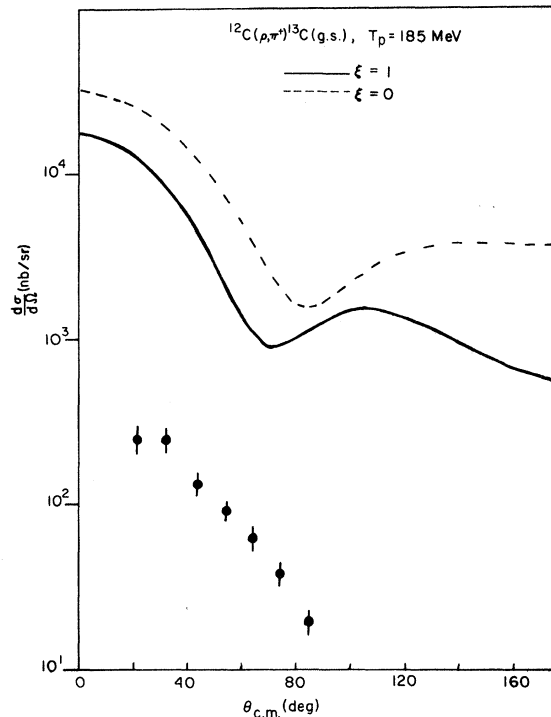Figure 1 is a plot of the calculated and experi-

mental differential cross sections vs the center-of-mass angle for the reaction ^{12}C$(p,\,\pi^+)^{13}$C$_{\text{g.s.}}$. The experimental data are those of Dahlgren et al.[5] The dashed and solid curves are the DWBA results using, respectively, Kisslinger ($\xi = 0$) and Kroll-Kisslinger ($\xi = 1$) wave functions for the pion distorted waves. The DWBA cross sections are 1 to 2 orders of magnitude higher than the experimental data at forward angles, and the calculated backward-angle cross section does not fall off as fast as the experimental cross section. These DWBA cross sections are also 2 to 3 orders of magnitude higher than cross sections calculated with proton distorted waves, and pion plane waves. Further, the μ/m term in the transition operator can be turned off with negligible effect on the calculated cross section.

Figure 2 is a plot of the calculated and experimental differential cross sections vs the center-of-mass angle for the reaction ^{12}C$(p,\,\pi^+)^{13}$C*$(3$–4 MeV) at $T_p = 185$ MeV. The experimental data are again those of Dahlgren et al.[5] Kroll-Kisslinger ($\xi = 1$) distorted waves were used in the DWBA
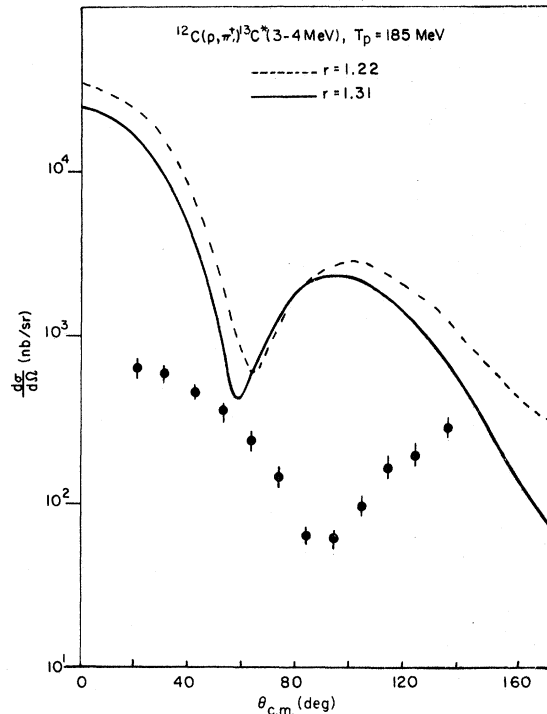

FIG. 1. This figure is a plot of the ^{12}C$(p,\pi^+)^{13}$C(g.s.) differential cross section vs the center-of-mass angle. The dashed curve is the DWBA result using the Kisslinger model ($\xi = 0$), and the solid curve is the DWBA result using the Kroll-Kisslinger model ($\xi = 1$). The experimental data are those of Dahlgren et al. (Ref. 5).

FIG. 2. This figure is a plot of the ^{12}C$(p,\pi^+)^{13}$C*$(3$–4 MeV) differential cross section vs the center-of-mass angle. The data are those of Dahlgren et al. (Ref. 5). The DWBA curves are calculated assuming ^{13}C is in the $\frac{1}{2}^+$ state at 3.09 MeV. The dashed curve was calculated using a radius of $R_n = 1.22A^{1/3}$ fm for the neutron (Woods-Saxon) potential. The solid curve had a radius of $R_n = 1.31A^{1/3}$ fm.

calculation, and it was assumed that ^{13}C was left in the $\frac{1}{2}^+$ state at 3.09 MeV. Different bound-state wave functions were used in order to test the sensitivity of the calculation to changes in this wave function. If the Woods-Saxon radius parameter is set at $R_n = 1.31A^{1/3}$ fm, then the calculated cross section is 1.0 to 1.4 orders of magnitude too high in the forward direction. The calculated cross section exhibits a minimum at 60°, and a second maximum at 97°, while the data appear to be symmetric about a minimum at 90°. If the Woods-Saxon radius parameter is set at $R_n = 1.22$ $A^{1/3}$ fm, then the calculated cross section is shifted up slightly, and the minimum and maximum are shifted out 3 to 4°. (If one assumes that ^{13}C is left in the $\frac{5}{2}^+$ state at 3.85 MeV, then the Kroll-Kisslinger cross section is 2.5 orders of magnitude higher than the data at forward angles, and 1.5 orders of magnitude too high at backward angles. Again the calculations are only moderately sensitive to changes in the neutron's wave function.)

The most striking effect in the above calculations is that the use of Kisslinger or Kroll-Kisslinger distorted waves results in DWBA cross sections which are at least an order of magnitude higher

than the data. This effect is consistent with the DWBA results of Jones and Eisenberg[6] who studied ^{12}C$(\pi^+, p)^{11}$C at an incident pion kinetic energy of 50 MeV, and compared their calculated cross section with the single experimental data point available. They pointed out that it is the velocity-dependent term in the Kroll-Kisslinger optical model which is responsible for the "unwanted overenhancement" in the DWBA cross sections. The unwanted overenhancement in the (p, π^+) DWBA cross sections, and presumably in the (π^+,p) DWBA cross sections, is caused predominately by the real part of the velocity-dependent term, as the imaginary part can be turned off with negligible effect. This rules out the possibility that the overproduction is being caused by an effectively positive imaginary contribution from the velocity-dependent term. Figure 3 shows the DWBA pion-production cross section calculated with the velocity-dependent term turned off ($b_1 = 0$). The parameter b_0 was adjusted to $b_0 = -6.41 + i7.29$. At forward angles, the order of magnitude and shape fits are relatively good for both the ground-state case,
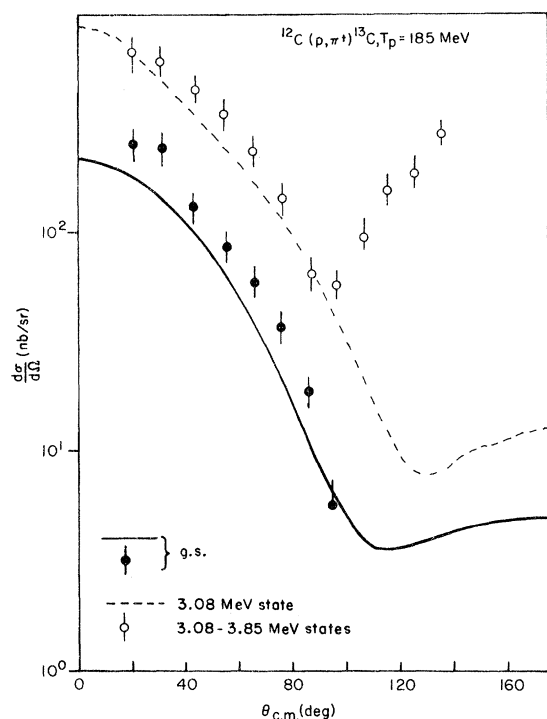

FIG. 3. This figure is a plot of the ^{12}C$(p, \pi^+)^{13}$C differential cross section vs the center-of-mass angle. The data are those of Dahlgren et al. (Ref. 5). The DWBA curves were calculated with a local potential ($b_1 = 0$). The parameter b_0 was $b_0 = -6.41 + i7.29$. For the excited-state curve, ^{13}C was assumed to be in the $\frac{1}{2}^+$ state at 3.09 MeV.
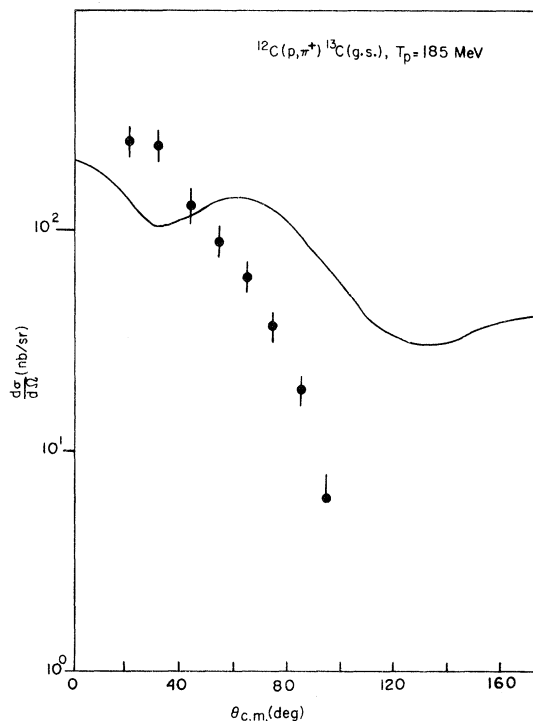

FIG. 4. This figure is a plot of the ^{12}C$(p, \pi^+)^{13}$C(g.s.) differential cross section vs the center-of-mass angle. The data are those of Dahlgren et al. (Ref. 5). The DWBA was calculated with different local potentials $V_l = d_l \rho(r)$ for each partial wave. The density was a modified Gaussian form, and the d's were adjusted to fit elastic scattering data.

and the excited-state case (assumed to be $\frac{1}{2}^+$ at 3.09 MeV). However, the excited-state backward-angle cross sections are not reproduced. Further, the distorted waves calculated in this way do not fit pion elastic scattering data. Note that, unlike the data, the two calculated curves behave roughly the same way at backward angles. This was typical of these calculations, and indicates that the physical effect responsible for the backward-angle cross sections has not been correctly included in these calculations.

In order to test whether the unwanted overenhancement is a result of the Kisslinger model, or is a result of all wave functions which fit pion elastic scattering, we replaced the Kisslinger potential with local complex potentials $V_l = d_l \, \rho(r)$, which were different for each partial wave. The parameters d_l were adjusted to fit the elastic scattering data. Figure 4 is a plot of the results using a modified Gaussian density, $\rho(r) = A(1 + Wr^2/a^2)e^{(-r^2/a^2)}$, where $A = 13$, $W = \frac{4}{3}$, and $a = 1.6$ fm. The d_l's which fit the elastic scattering data were:

$d_0 = 1.8 - i\,0.02$ MeV; $d_l = -3.8 - i\,0.18$ MeV for $l \geqslant 1$. The calculated result is now roughly the same order of magnitude as the data at forward angles (less than a factor of 3 different from 0 to 75°). However the backward-angle cross section is at least a factor of 10 too high. We also used Woods-Saxon densities with various parameters and the results were similar, although the shapes of the curves are more diffraction-like. Numerical comparison of these wave functions with Kroll-Kisslinger wave functions supports an argument by Eisenberg[7] that the Kisslinger model results in an abnormally high pion effective momentum inside the nucleus. Therefore, if the reaction takes place inside the nucleus, the effective momentum transfer is smaller and the resulting cross sections are enhanced.

Figure 5 is a plot of the total pion-production cross section σ_{tot} calculated as a function of the incident proton kinetic energy T_p for the case where ^{13}C is left in the ground state. The experimental value is 580 nb. (This value was obtained by extrapolating back to 0°, and then integrating.) Three curves are shown. The dot-dashed curve was calculated with Kroll-Kisslinger pion wave functions. For this case, the potential parameters were varied in a smooth way to simulate energy dependence. The resulting σ_{tot} is a factor of 37 larger than the experimental data point at $T_p = 185$ MeV, and shows a steady increase as T_p is increased to 240 MeV. The solid curve was calculated with the local potential used for Fig. 3 ($b_0 = -6.41 + i\,7.29$, $b_1 = 0$). At $T_p = 185$ MeV, the resulting σ_{tot} is less than a factor of 1.2 below the experimental data point. In contrast to the Kroll-Kisslinger curve, this curve rises only slightly as T_p is increased to 240 MeV. For $T_p < 156$ MeV the local-potential curve begins to decrease rapidly as T_p decreases toward threshold. The dashed curve is the result of a full plane-wave calculation. It is only slightly smaller (30 nb) than the local potential curve at $T_p = 185$ MeV, and remains relatively constant as T_p increases from 185 to 240 MeV. As T_p decreases from 185 MeV to threshold, the plane-wave curve falls off faster than the local-potential curve, so that at 156 MeV it is a factor of 2 smaller.

Limited success was obtained with this approximation only when the velocity-dependent term in the Kisslinger model was discarded ($b_1 = 0$). It appears that the Kisslinger-type pion waves are incorrect inside the nucleus even though they are correct outside the nucleus (they give phase shifts which fit the elastic scattering data). Therefore there is a need for an improved pion optical model. With improved pion distorted waves and a more sophisticated production mechanism (pion able to
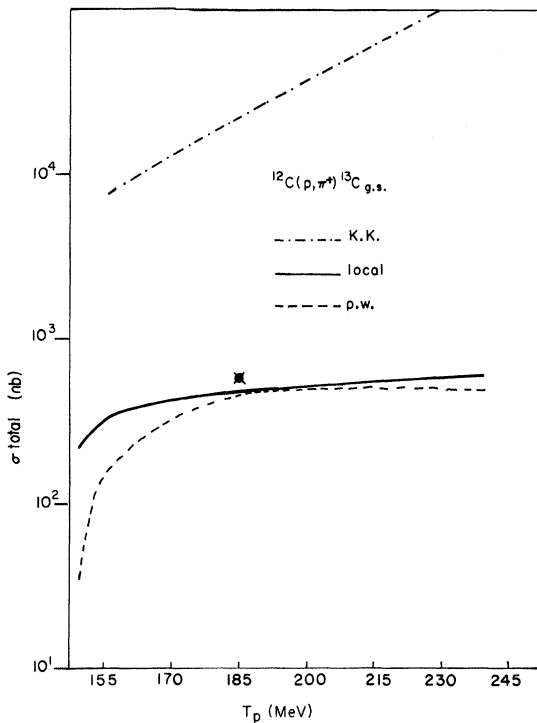
FIG. 5. This figure is a plot of the ^{12}C$(p,\pi^+)^{13}$C(g.s.) total cross section as a function of the incident proton kinetic energy, T_p. The experimental value at $T_p = 185$ MeV is 580 nb. The dot-dashed curve was obtained using Kroll-Kisslinger pion waves. The solid curve was obtained using a local potential with $b_0 = -6.41 + i7.29$, $b_1 = 0$. The dashed curve was obtained with plane waves for both the pion and the proton. The neutron's bound-state wave function was the same for all three cases.

be emitted either by the incident proton, or by one of the nucleons in the nucleus), DWBA may be an inadequate approximation for this high-momentum-transfer reaction. We would like to see further pion-production experiments on other nuclei in order to see if the striking difference between

the ground-state cross section, and excited-state cross section is characteristic of nuclei besides ^{13}C. It would also be very useful to have pion-nucleus elastic data for the residual nucleus (^{13}C in this case).

[1]A. Johannsson, U. Svanberg, and P. E. Hodgson, Arkiv Fysik 19, 541 (1961).

[2]L. Kisslinger, Phys. Rev. 98, 761 (1955).

[3]See Ref. 18, Phys. Rev. 122, 252 (1961).

[4]J. F. Marshall, M. E. Nordberg, and R. L. Burman, Phys. Rev. C 1, 1685 (1970).

[5]S. Dahlgren, P. Grafstrom, B. Hoisted, and A. Asberg, talk presented at the Fourth International Conference on High Energy Physics and Nuclear Structure, Dubna, USSR, 1971 (unpublished).

[6]W. B. Jones and J. M. Eisenberg, Nucl. Phys. A154, 49 (1970).

[7]J. M. Eisenberg, Seminar, Indiana University, 1971 (unpublished).

Center-of-Mass Motion in Many-Particle Systems.
II. Critique of the Gartenhaus-Schwartz Transformation*

D. J. Ernst, C. M. Shakin, and R. M. Thaler

Physics Department, Case Western Reserve University, Cleveland, Ohio 44106

(Received 1 December 1972)

We examine the Gartenhaus and Schwartz (G-S) transformation, which generates a translationally invariant wave function from one which does not possess this property. A clarification of the G-S procedure for the calculation of matrix elements is achieved if one takes two independent limits of the parameters Λ, Λ' which appear in the expression for a transformed operator $\vec{a}' = (\lim_{\Lambda' \to \infty} U_{\Lambda'}^{\dagger})\, \vec{a}\, (\lim_{\Lambda \to \infty} U_{\Lambda})$. It is shown that the G-S operator, $U = \lim_{\Lambda \to \infty} U_{\Lambda} = \lim_{\Lambda \to \infty} \exp[-\frac{1}{2} i \Lambda (\vec{R} \cdot \vec{P} + \vec{P} \cdot \vec{R})]$, is equivalent to the operator $U = (2\pi)^3 \delta(\vec{P}) \delta(\vec{R})$. This operator is seen to be a specific example of the more general class of operators presented earlier.

In the work of Gartenhaus and Schwartz[1] (G-S) an operator is presented which transforms any wave function into one which is translationally invariant. If we are given a many-particle function,

$$\Phi(\vec{r}_1, \vec{r}_2, \dots, \vec{r}_A) \equiv \Phi(\vec{r}_i), \tag{1}$$

which depends on the particle coordinates $\vec{r}_i$, then a new function Ψ may be generated therefrom by a transformation

$$\Psi = U\Phi, \tag{2}$$

such that Ψ has the property

$$\Psi(\vec{r}_i + \vec{\Delta}) = \Psi(\vec{r}_i) \tag{3}$$

for arbitrary $\vec{\Delta}$. Such a Ψ is generated by the G-S

operator U, defined as

$$U \equiv \lim_{\Lambda \to \infty} e^{-(i/2)\Lambda(\vec{R} \cdot \vec{P} + \vec{P} \cdot \vec{R})}, \tag{4}$$

with $\vec{R}$ the center-of-mass operator and $\vec{P}$ the total momentum operator.

Now, following G-S, let us consider the calculation of a matrix element of an operator Θ,

$$\Theta_{fi} \equiv \langle \Psi_f | \Theta | \Psi_i \rangle, \tag{5}$$

which, because of Eq. (3), can be written in the form

$$\Theta_{fi} \equiv \langle \Phi_f | \Theta' | \Phi_i \rangle = \langle \Phi_f | (\lim_{\Lambda' \to \infty} U_{\Lambda'}^{\dagger}) \Theta (\lim_{\Lambda \to \infty} U_{\Lambda}) | \Phi_i \rangle. \tag{6}$$

Let us follow G-S further and investigate the trans-